Available online at www.sciencedirect.com
ScienceDirect
Ceramics International 37 (2011) 935–942
CERAMICS INTERNATIONAL
www.elsevier.com/locate/ceramint

Enhanced phase stability in hydroxylapatite/zirconia composites with hot isostatic pressing

Celaletdin Ergun *

Istanbul Technical University, Department of Mechanical Engineering, Beyoğlu 34437, Istanbul, Turkey

Received 18 August 2010; received in revised form 13 October 2010; accepted 29 October 2010
Available online 2 December 2010

Abstract

Hydroxylapatite (HA) composites with pure zirconia (ZrO_2), and 3 and 8% Y_2O_3 doped ZrO_2 were pressure-less sintered in air and hot isostatically pressed (under 120 MPa gas pressure) at 1100 °C for 2 h. The reactions and phase transformations were monitored by X-ray diffraction, thermal analysis, and Raman spectroscopy. HA/pure ZrO_2 composites were not thermally stable in air sintering; HA dissociated into α and β tricalcium phosphate while monoclinic ZrO_2 was transformed into tetragonal and cubic phases. No decomposition in HA or phase transformation in ZrO_2 were observed in hydroxylapatite/3% Y_2O_3 doped ZrO_2 or HA/8% Y_2O_3 doped ZrO_2 composites. On the other hand, HA and ZrO_2 phases in hot isostatically pressed composites remained stable. The highest densification was found in a composite initially containing 10% monoclinic ZrO_2 among the composites sintered in air. The densification of the composites decreased at lower sintering temperatures and higher ZrO_2 contents upon air-sintering. The HIPped composites were densified to about 99.5% of theoretical densities in all mixing ratios. The reactivity between ZrO_2 and HA was dependent on the amount of air in the sintering environment. Hot isostatic pressing with very limited retained air was proved to be a very convenient method to insure both phase stability and full densification during the production of hydroxylapatite zirconia composites.

Keywords: Biomedical applications; Hot isostatic pressing; Sintering; Powders: solid state reaction

1. Introduction

The chemical composition of synthetic hydroxylapatite (HA) is very close to that of the inorganic component of bone. The implants made of HA are accepted by human body promoting bone growth on its surface, thus bonding physico-chemically with bone [1]. However, its brittleness and low tensile strength are the main drawbacks for load bearing implant applications. Therefore, HA coatings on metals or HA based composites have been introduced to improve the mechanical properties of HA [2–5].

HA and tetragonal zirconia composites have shown promising improvements in the strength and toughness as compared to monolithic HA, and thus taking the advantages of both the biocompatibility of HA and the high mechanical properties of tetragonal zirconia in the same material [6–12]. However, these composites can suffer from the decomposition of HA into second phases and the phase transformation of partially stabilized zirconia from tetragonal to cubic phase during sintering in air, resulting in a decrease of both the mechanical properties and the biocompatibility.

The reason for the phase transformations in zirconia and the decomposition of HA is attributed to Ca^{2+} diffusion from HA to zirconia, which is active at temperatures lower than the decomposition temperature of pure HA and the air sintering temperatures of composites [7–15]. Many efforts have been made to increase the thermal stability of both phases during processing. Among them, CaF_2 [16], MgO and MgF_2 [17], YF_3 [18], and ZrF_4 [19] were added in small amounts to enhance the phase stability of HA and zirconia during processing. Other efforts were mainly focused on pressure sintering methods, such as hot isostatic pressing (HIP) and hot pressing (HP), to reduce the sintering temperature and preserve both the HA and the ZrO_2 phases during sintering. However, there are still controversial results in the literature about the phase stability of these composites prepared by pressure sintering methods. Indeed, some reaction has been reported between HA and ZrO_2 by some researchers [12–14], but not by others [9,10]. However

* Tel.: +90 533 653 1988; fax: +90 212 245 0795.
E-mail address: ergunce@itu.edu.tr.

0272-8842/$36.00
doi:10.1016/j.ceramint.2010.11.001

Table 1
Abbreviation and the composition of the samples.

Name	Abbreviation	Composition
Hydroxylapatite	HA	Pure
Zirconia	ZrO_2	100%
3 wt.% Y_2O_3 doped ZrO_2	YSZ3	100%
8 wt.% Y_2O_3 doped ZrO_2	YSZ8	100%
Hydroxylapatite–zirconia composites	$HAZrO_2$-10	90 wt.% HA + 10 wt.% ZrO_2
	$HAZrO_2$-25	75 wt.% HA + 25 wt.% ZrO_2
	$HAZrO_2$-35	65 wt.% HA + 35 wt.% ZrO_2
	$HAZrO_2$-50	50 wt.% HA + 50 wt.% ZrO_2
Hydroxylapatite–3 wt.% Y_2O_3 doped ZrO_2 composites	HAYSZ3-10	90 wt.% HA + 10 wt.% YSZ3
	HAYSZ3-25	75 wt.% HA + 25 wt.% YSZ3
	HAYSZ3-35	65 wt.% HA + 35 wt.% YSZ3
	HAYSZ3-50	50 wt.% HA + 50 wt.% YSZ8
Hydroxylapatite–8 wt.% Y_2O_3 doped ZrO_2 composites	HAYSZ8-10	90 wt.% HA + 10 wt.% YSZ8
	HAYSZ8-25	75 wt.% HA + 25 wt.% YSZ8
	HAYSZ8-35	65 wt.% HA + 35 wt.% YSZ8
	HAYSZ8-50	50 wt.% HA + 50 wt.% YSZ8

there is a common agreement that the composites were substantially stable especially after HIP [6–8], even though an increase in reactivity may be expected due to the increased contact area between HA matrix and dispersed ZrO_2 particles [8]. On the other hand, a partial reaction between HA and zirconia was observed in the composites prepared by hot pressing but still much less than observed in sintering in air [13,14]. These results suggest that the sintering environment may be an important parameter affecting the thermal stability of HA and ZrO_2 in the composites.

The purpose of the present study is to evaluate the effect of the sintering environment on the thermal stability and interactions between HA and zirconia in pressureless air sintering and sintering by HIP. The composites prepared were characterized by X-ray diffraction (XRD), thermal analysis, Raman spectroscopy, and sinterability.

2. Experimental procedures

HA was synthesized by the precipitation method [14]. Zirconia powders were supplied from a commercial source (Zirconia Sales Inc.). The powders of HA and the zirconias (ZrO_2; 3 mol.% Y_2O_3 doped ZrO_2; 8 mol.% Y_2O_3 doped ZrO_2) were mixed in desired weight ratios (Table 1).

HA powder was calcined at 900 °C for 2 h prior to mixing with the zirconias. This step is very important for evaporation

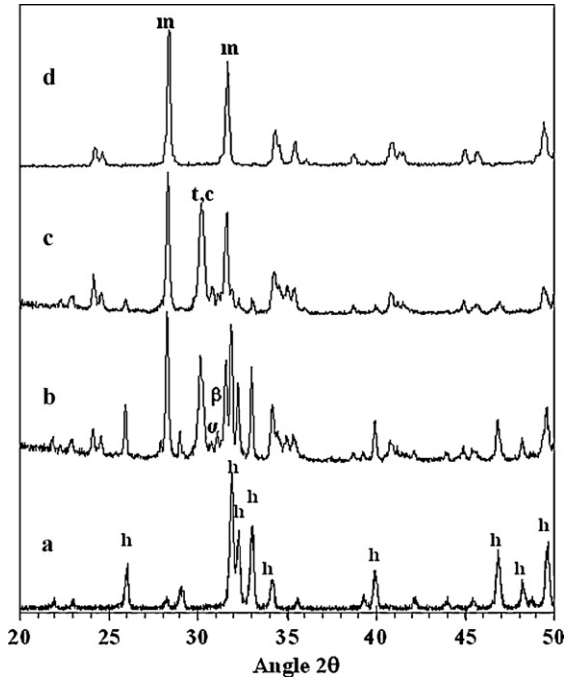

Fig. 1. XRD patterns of air-sintered composites at 1100 °C for 2 h: (a) HA, (b) $HAZrO_2$-25, (c) $HAZrO_2$-50, (d) ZrO_2 (t,c, tetragonal and/or cubic ZrO_2; α and β, tricalcium phosphate; m, monoclinic zirconia; h, hydroxylapatite).

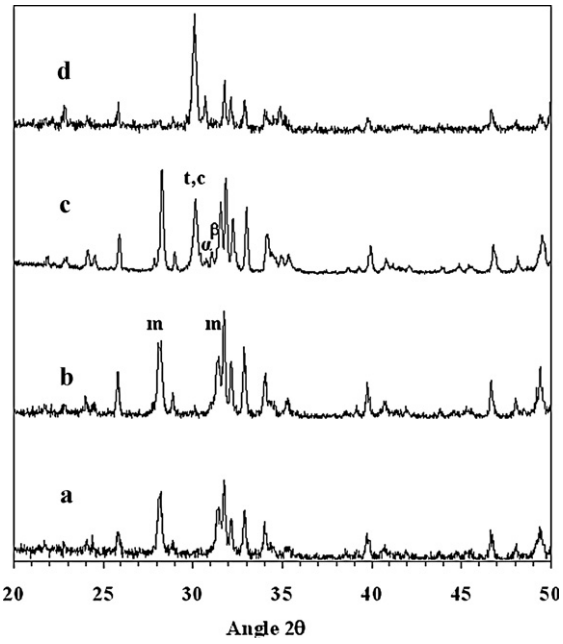

Fig. 2. XRD result of $HAZrO_2$-25 composites sintered for 2 h at (a) 900 °C, (b) 1000 °C, (c) 1100 °C, (d) 1200 °C. (t,c, tetragonal/cubic zirconia, m, monoclinic zirconia; α and β, tricalcium phosphate).

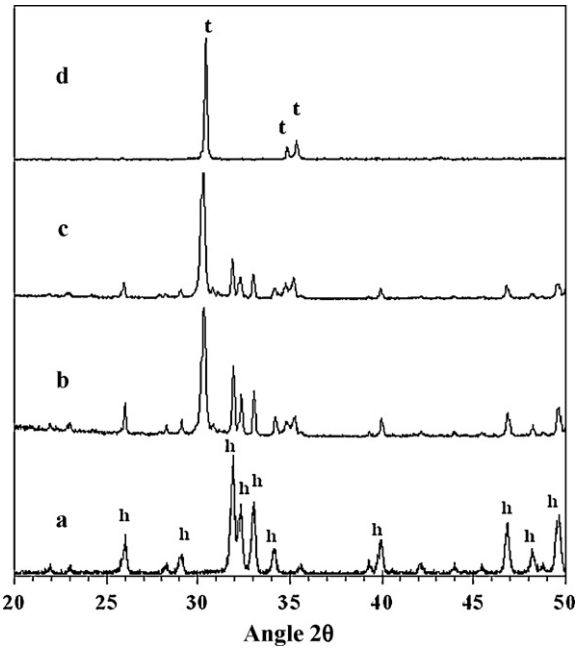

Fig. 3. XRD result of air-sintered HAYSZ3 composites at 1100 °C for 2 h: (a) HA, (b) HAYSZ3-25, (c) HAYSZ3-50, (d) YSZ3 (t, tetragonal zirconia, h, hydroxylapatite).

of the absorbed or excess amount of structural water of HA especially before HIPping to prevent the release of water vapor to cause explosion of the glass envelopes during HIPping. Then the calcined powders were mixed with the corresponding zirconia powder in the desired ratios (Table 1), homogeneously mixed by ball milling in an ethyl alcohol medium, and then quickly filtered through a fine filter paper to prevent segregation due to the density differences of the two components. The filtered cakes were kept at 200 °C overnight to remove the residual ethyl alcohol, then crushed and cold-pressed at 200 MPa in bar shaped green bodies 5 mm × 10 mm × 50 mm mm in size, that were sintered by: (a) pressureless air-sintering at the temperatures between 900 °C and 1200 °C for 2 h and (b) hot isostatic pressing, depending on the test protocol.

The green bodies prepared for HIP were coated with a boron nitride aerosol spray and placed into borosilicate glass tubes. The tubes were dried at 200 °C overnight and extra care was given to keep the samples as dried as possible without any residual moisture. Subsequently, the tubes were sealed under vacuum and placed into a graphite supporter and then into the HIP chamber (International Pressure Service). HIPping of the composites was performed at

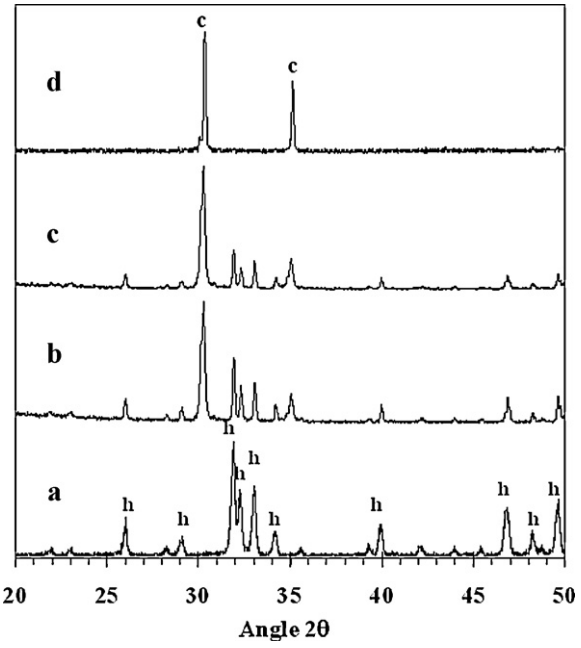

Fig. 4. XRD result of air-sintered HAYSZ8 composites at 1100 °C for 2 h: (a) HA, (b) HAYSZ8-25, (c) HAYSZ8-50, (d) YSZ8 (c, cubic zirconia; h, hydroxylapatite).

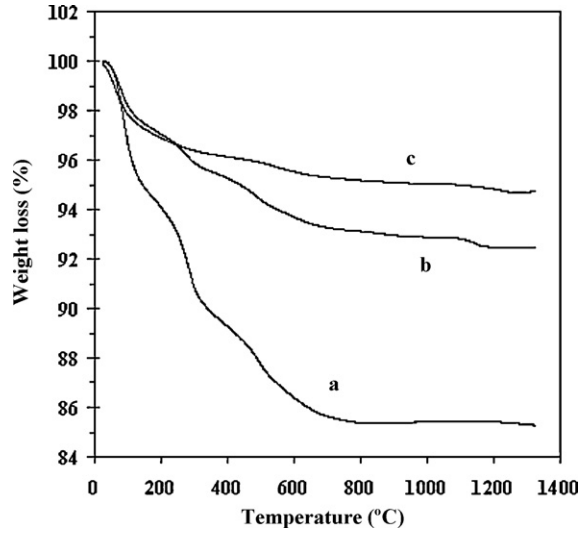

Fig. 5. TGA graphs: (a) pure HA, (b) $HAZrO_2$-25, (c) HAYSZ3-25.

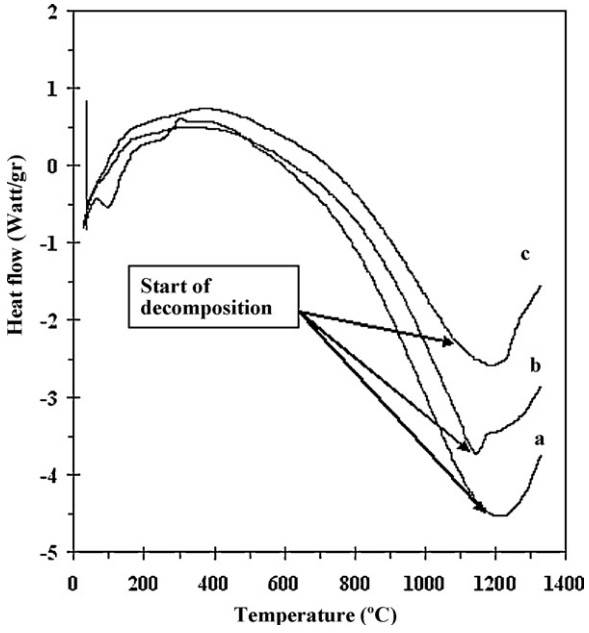

Fig. 6. DTA graphs where Watt/gr is Watt/grams: (a) Pure HA, (b) $HAZrO_2$-25, (c) HATSZ3-25.

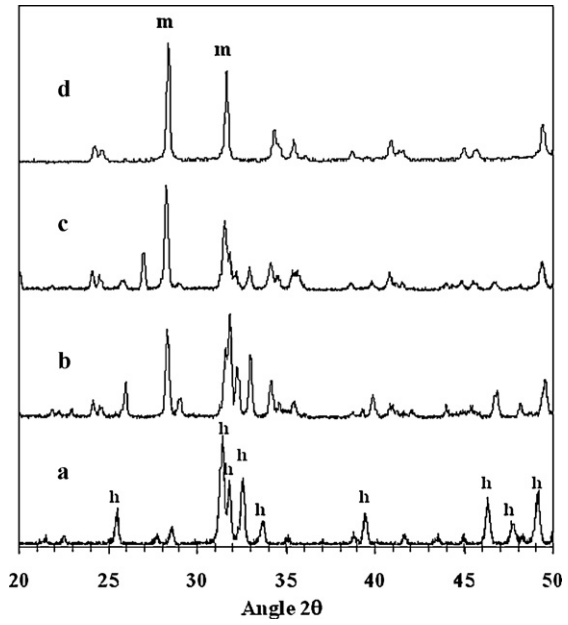

Fig. 7. XRD result of $HAZrO_2$ composites HIPped at 120 MPa, 1100 °C for 2 h: (a) pure HA, (b) $HAZrO_2$-25, (c) $HAZrO_2$-50, (d) pure zirconia (m, monoclinic zirconia; h, hydroxylapatite).

1100 °C and 120 MPa for 2 h. Heating and cooling rates were maximum 500 °C/h.

The XRD patterns of the pure HA, ZrO_2 were used to identify the reactions and structural changes during sintering. XRD were carried out using a Scintag Inc XRD unit operating with Ni filtered Cu Kα radiation. XRD spectra were collected at 2θ angles between 20° and 70° with 0.02°/min scan speed at 40 kV/30 mA.

The thermal analysis of pure HA, $HAZrO_2$-25 and HAPSZ3-25 samples were performed in a TA Instruments SDT 2960 TGA system at a 20 °C/min heating/cooling rate from RT to 1350 °C under 100 mL/min air purge.

A Renishaw Ramanscope System 2000 connected to a 514 nm Argon ion laser was used to record the Raman spectra of the composites. The surfaces of the composite samples used for the measurements were polished with a 0–1 μm diamond finish. The laser beam was focused to a spot on the surfaces using a modified Olympus microscope. The measurements were performed at 50× microscope magnifications. Raman spectra were recorded using a charge coupled device (CCD). Raman spectra were recorded at periodic time intervals in which the time required to record a single measurement was 10 s and the total number of scans was 10 for each measurement.

The density of the samples was calculated by dividing the weight by its volume [14].

3. Results

XRD patterns of air sintered $HAZrO_2$ composites are given in Fig. 1. The change in relative XRD intensities of the zirconias and HA bears two information: (a) the corresponding changes in the weight ratio of zirconia to HA in the composite and (b) the possible phase transformations during processing. Sintering in air at 1100 °C leads the monoclinic ZrO_2 to partially transform to tetragonal and/or cubic ZrO_2 and certain amount of HA to partially decompose to a mixture of α and β tricalcium phosphate (TCP) in an agreement with Ref. [15]. While pure HA starts to decompose thermally above 1300 °C depending on the partial vapor pressure of water [14,15], HA in $HAZrO_2$ composites

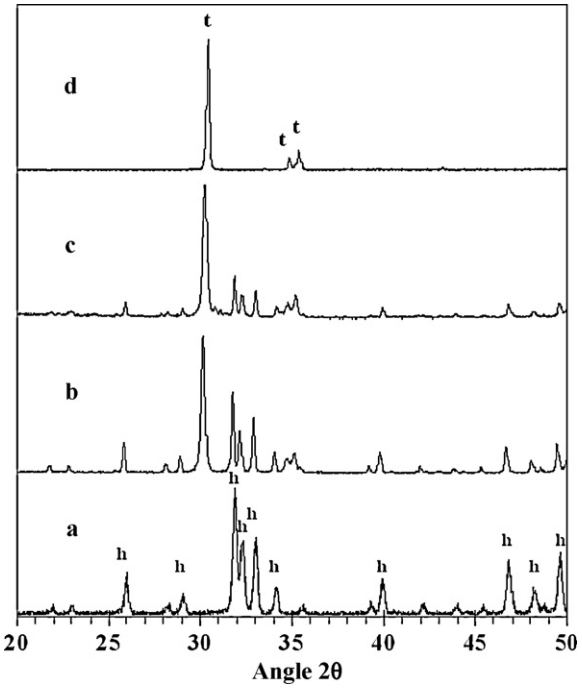

Fig. 8. XRD result of HAYSZ3 composites HIPped at 120 MPa, 1100 °C for 2 h: (a) pure HA, (b) HAYSZ3-25, (c) HAYSZ3-50, (d) pure YSZ3 (t, tetragonal zirconia; h, hydroxylapatite).

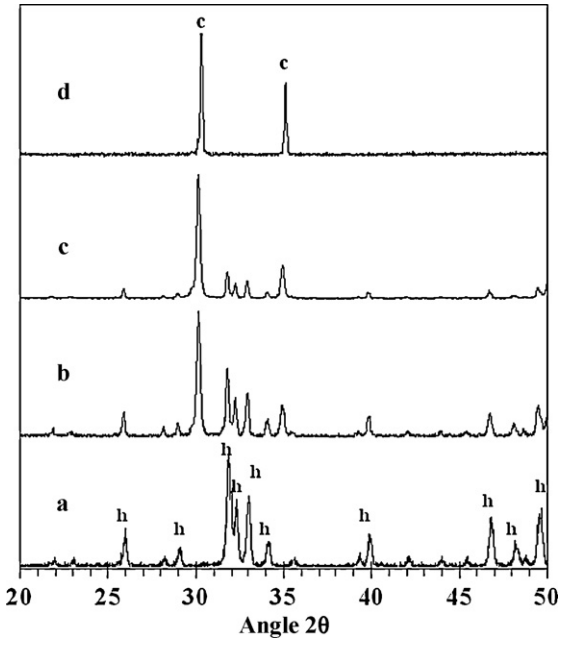

Fig. 9. XRD result of HAYSZ8 composites HIPped at 120 MPa, 1100 °C for 2 h: (a) pure HA, (b) HAYSZ8-25, (c) HAYSZ8-50, (d) YSZ8 (c, cubic zirconia; h, hydroxylapatite).

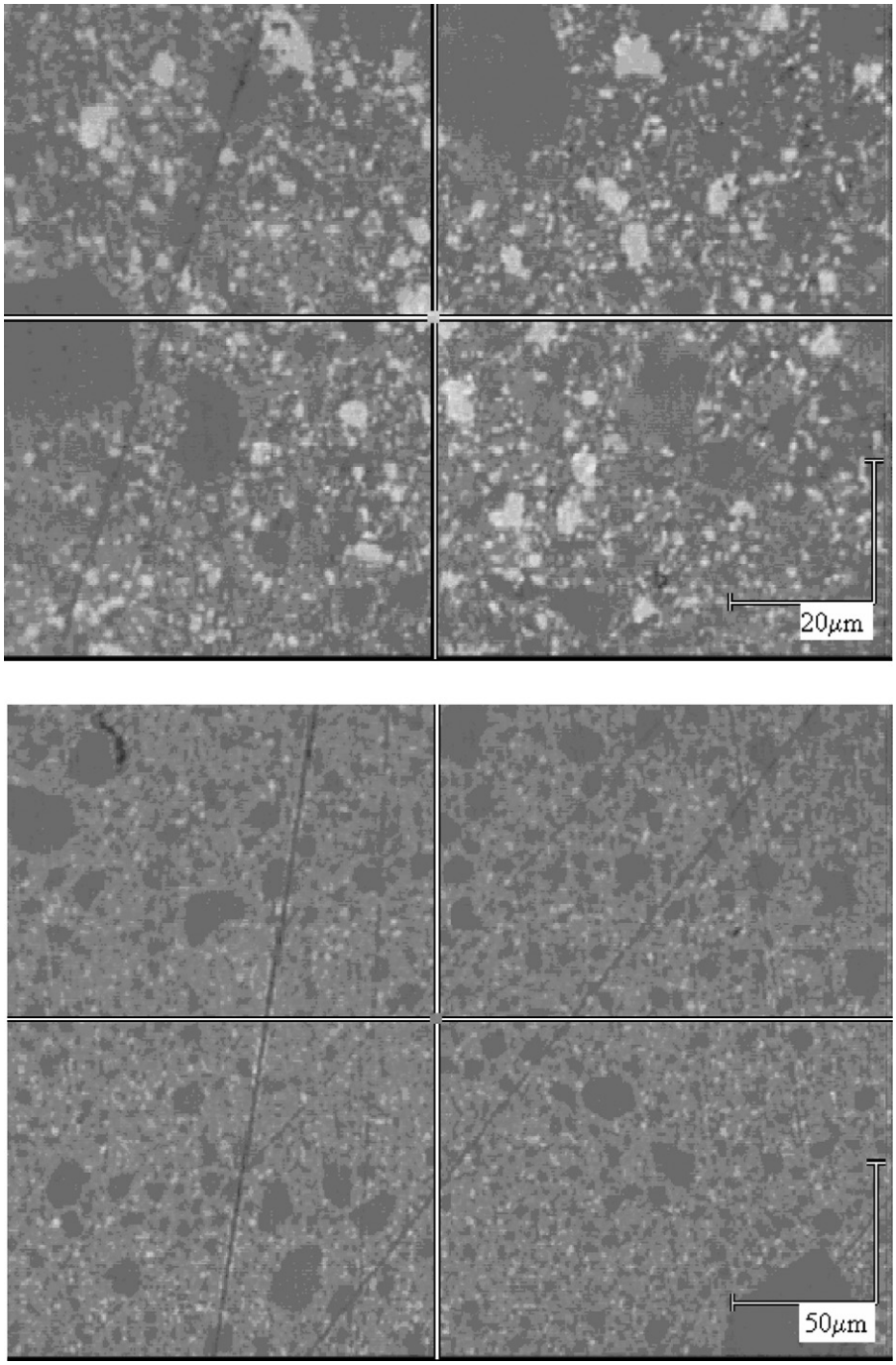

Fig. 10. Optic micrographs of composites HIPped at 120 MPa, 1100 °C for 2 h: $HAZrO_2$-25 and HAYSZ3-25.

decomposed at lower temperatures, which seems to be accelerated by chemical interaction between the phases.

X-ray diffraction patterns of $HAZrO_2$-25 pellets sintered for 2 h at temperatures between 900 and 1200 °C are given in Fig. 2. As the sintering temperature increased the monoclinic ZrO_2 began to transform to tetragonal or cubic ZrO_2 at 1100 °C, and the transformation completed at 1200 °C. HA began to decompose to a mixture of α and β tricalcium phosphate (TCP) at 1100 °C; this decomposition was nearly complete at 1200 °C, and the TCP was entirely α phase.

XRD patterns of HAYSZ3 and HAYSZ8 composites air sintered at 1100 °C for 2 h are shown in Figs. 3 and 4, respectively. The XRD peaks were a superposition of the patterns of HA and YSZ3 or HA and YSZ8 depending on their weight ratios in the respected composites. No significant phase transformations or second phases were detected in these composites and both HA and zirconia were stable compared to $HAZrO_2$ composites.

The results of TGA and DTA are shown in Figs. 5 and 6, respectively, for the pure HA, $HAZrO_2$-25 and HAYSZ3-25 composites. TGA curve indicated a continuous weight loss up to about 1100 °C. Relatively major weight loss, Fig. 6, occurred between 20 and 200 °C most probably due to the evaporation of this absorbed water during synthesis (Fig. 5).

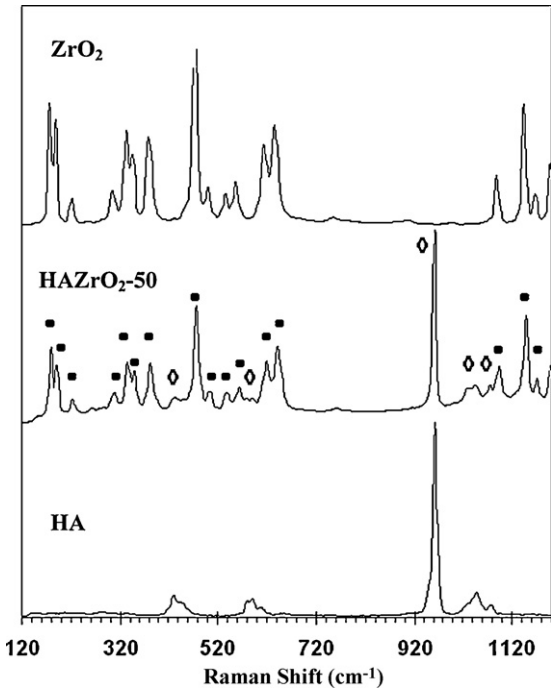

Fig. 11. Raman spectra of pure HA, $HAZrO_2$-50 HIPped at 120 MPa, 1100 °C for 2 h, monoclinic ZrO_2 (●: monoclinic zirconia and ◇: HA).

Further heating yielded a progressive loss between 200 °C and 900 °C [14].

The endothermic peak near 1250 °C in the DTA may reflect the starting point for decomposition of pure HA. On the other hand, this peak shifted to near 900 °C for $HAZrO_2$-25 and 1150 °C for HAYSZ3-25 composites. Higher loss of water in $HAZrO_2$-25 compared to HAYSZ3-25 seems to be due to the higher reactivity between HA and pure ZrO_2 compared to HA and YSZ3 or HA and YSZ8. This finding is also supported by the XRD results given in Fig. 2, where tetragonal/cubic peak of zirconia appeared in the samples sintered at 1000 °C. The transformation became more pronounced in the samples sintered at 1100 °C.

The XRD patterns of $HAZrO_2$ composites HIPped at 1100 °C and 120 MPa for 2 h are presented in Fig. 7. Compared to the air-sintered composites (Fig. 1), there was no decomposition or second phases for the same sintering temperature and both HA and zirconia phases remained stable. Similarly, the HA and zirconia were also stable in HIPped HAYSZ3 and HAYSZ8 composites as shown in Figs. 8 and 9, respectively.

Optical micrographs of the surfaces of the HIPped composites on which Raman analyses were performed are presented in Fig. 10. Raman spectra of the $HAZrO_2$-25 and HAYSZ3-25 are given in Figs. 11 and 12, respectively. The frequencies of monoclinic and tetragonal ZrO_2 and HA agree well with those reported in the literature [20–23]. The spectra for the composite sample show that peaks the structures of HA and monoclinic zirconia were preserved after HIPping and no other peaks were identified.

The relative density of the composites is shown in Fig. 13 for both air sintered and HIPped conditions. The maximum attainable density was about 70% for $HAZrO_2$-10 sample. Near full density (99.5% of theoretical density) was obtained in the HIPped composites.

4. Discussion

The monoclinic phase transformed to tetragonal or cubic form during air sintering at 1100 °C in HA/monoclinic ZrO_2 composites (Fig. 1). Since the effective solubility of CaO in ZrO_2 at 1100 °C is about 17.5 mol.% [12], monoclinic ZrO_2 can uptake and solve CaO from HA by diffusion and therefore possibly act as a catalyst for the decomposition of HA as a consequence of its CaO loss. Normally, thermal decomposition

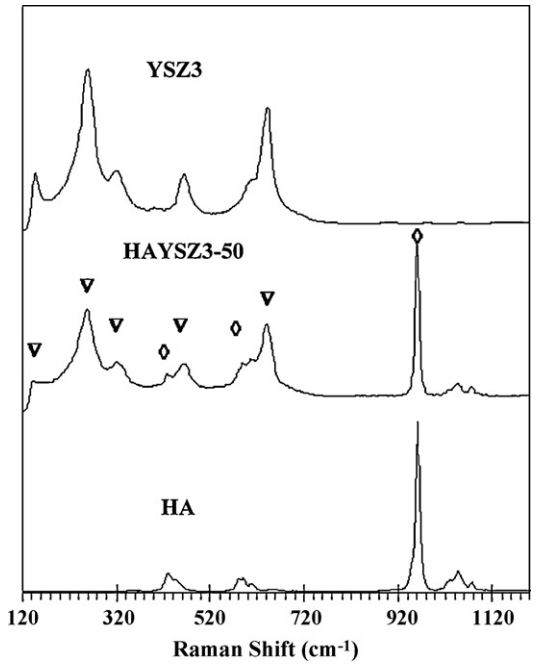

Fig. 12. Raman spectra of HA, HAYSZ3-50 HIPped at 120 MPa, 1100 °C for 2 h, YSZ3 (▽: tetragonal zirconia and ◇: HA).

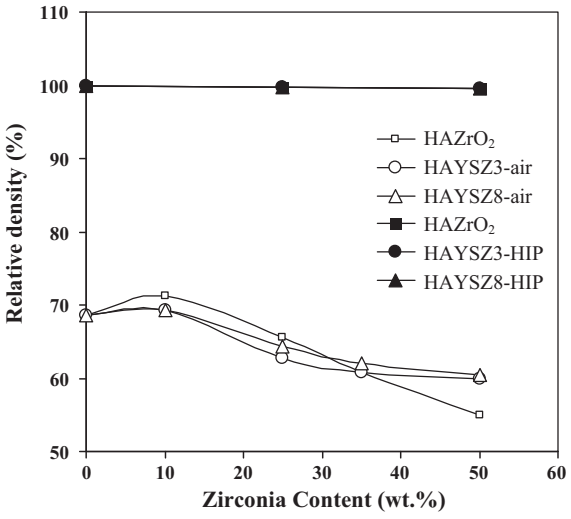

Fig. 13. Relative density as a function of the amount of monoclinic, tetragonal or cubic zirconia phase in composites.

of HA occurs above 1300 °C depending on the sintering atmosphere. However, in the presence of monoclinic zirconia, decomposition of HA happens as low as 900–1000 °C with the following reactions:

$$Ca_{10}(PO_4)_6(OH)_2 \rightarrow 3Ca_3(PO_4)_2 + CaO + H_2O \quad (1)$$

$$Ca_{10}(PO_4)_6(OH)_2 + (ZrO_2)m \rightarrow [CaO{-}ZrO_2]t,c + 3Ca_3(PO_4)_2 + H_2O \quad (2)$$

The release of water as byproduct of this reaction causes the formation of porosity in the sintered composites and may also play a major role in the lower sinterability especially in air-sintering conditions [14].

No decomposition in HA composites with ZrO_2 containing 3 or 8 mol.% Y_2O_3 was detected compared to those with pure monoclinic ZrO_2, possibly due to the slower diffusion of CaO in the ZrO_2 due to the barrier effect of Y_2O_3 [14].

No detectable second phases or transformations in monoclinic or tetragonal ZrO_2 were observed in the XRD and Raman analysis of the HIPped composites. This is supposed to be a consequence of the prevention of water release, as the byproduct (Eq. (1)), from HA in the composites due to the utilization of an airtight glass encapsulation in HIPping [9]. This may explain why HA dissociates during air-sintering, in which there is no any confinement for released water. However, it does not explain why HA underwent a lesser amount of dissociation, in HA/zirconia composites during hot pressing, compared to air sintering [13,14], in which the water release from the HA in composite should freely take place. Therefore, it seems to be difficult to explain the stability of HA and ZrO_2 during HIPping just relating to the prevention of water loss, and supposedly inhibition of Ca diffusion from HA to ZrO_2.

Additionally, it should be noted that the amount of air and/or moisture present in the sintering environment would be another major difference between HIP and air sintering or hot pressing processes. In the evacuated and sealed glass tube used in HIP, the air/moisture content is very limited. However, hot pressed chamber, which may be vacuumed or filled/circulated inert gas atmosphere, may contain air/moisture contaminations and thus may introduce more atomic species to the processing environment.

It should also be taken into account that preserving the ionic charge balance in the diffusing species during the diffusion/reaction in the metal/ceramic and ceramic/ceramic couples [24–26], should also play an important role at the HA/ZrO_2 interface. Consequently, the diffusion of Ca from HA to ZrO_2 may also be a complicated process and may have intermediate reduction/oxidation steps. For instance, charge balance may be preserved with the diffusion of ZrO^{2+} ions into HA lattice from ZrO_2 at the interface while Ca was diffusing from HA to ZrO_2 as reported in Ref. [13].

In this extent, it may be speculated that the combination of the atomic species in moisture/air such as oxygen, hydrogen, and carbon dioxide, may play a role in the reduction/oxidation of the diffusing species at the HA/ZrO_2 interface to satisfy the charge balance and promote a subsequent Ca diffusion from HA to ZrO_2 just like in air sintered samples. Since much lesser amount of air/moisture may exist in the form of contamination in hot pressing, Ca diffusion from HA to ZrO_2 and the following decomposition in HA and transformation in ZrO_2 was limited compared to air sintering. Clearly more researches are needed to develop a complete understanding on the effect of the sintering environment on the phase stability of both HA and ZrO_2.

While as a general trend the density of air sintered composites decreased as the zirconia phase increased in the air sintered composites, near full density was attained in the HIPped composites.

5. Conclusions

The thermal phase stability in hydroxylapatite/zirconia composites produced with air sintering and HIPping was studied. Hydroxylapatite started decomposing in the presence of monoclinic zirconia when sintered in air at 1000 °C, while monoclinic zirconia transformed to the tetragonal/cubic phase. The reactivity between hydroxylapatite and zirconia was primarily related to the effect of air in the sintering environment. No decomposition in hydroxylapatite or phase transformation in zirconia phases was observed when HIPped at 1100 °C, 120 MPa, with very limited retain air in its closed system. Therefore this method is a very convenient one to get fully densified HA–zirconia composites at temperatures lower than the thermal decomposition of HA.

References

[1] B.M. Tracy, R.H. Doremus, Direct electron-microscopy studies of the bone–hydroxylapatite interface, J. Biomed. Mater. Res. 18 (1984) 719.
[2] A.K. Lynn, D.L. DuQuesnay, Hydroxyapatite-coated Ti–6Al–4V. 1. The effect of coating thickness on mechanical fatigue behaviour, Biomaterials 23 (9) (2002) 1937–1946.
[3] C. Massaro, M.A. Baker, F. Cosentino, P.A. Ramires, S. Klose, E. Milella, Surface and biological evaluation of hydroxyapatite-based coatings on titanium deposited by different techniques, J. Biomed. Mater. Res. 58 (6) (2001) 651–657.
[4] S. Deb, M. Wang, K.E. Tanner, W. Bonfield, Hydroxyapatite polyethylene composites: effect of grafting and surface treatment of hydroxyapatite, J. Mater. Sci.: Mater. Med. 7 (1996) 191.
[5] K. Kangasniemi, K. Degroot, J. Wolke, O. Andersson, Z. Luklinska, J.G.M. Bencht, Z. Lakkisto, A. Yli-Urpo, The stability of hydroxyapatite in an optimized bioactive glass matrix at sintering temperatures, J. Mater. Sci.: Mater. Med. 2 (1991) 133.
[6] M. Takagi, M. Mochida, N. Uchida, K. Saito, K.J. Uematsu, Filter cake forming and hot isostatic pressing for tzp-dispersed hydroxyapatite composite, J. Mater. Sci.: Mater. Med. 3 (1992) 199.
[7] J.M. Wu, T.S. Yeh, Sintering of hydroxylapatite zirconia composite-materials, J. Mater. Sci. 23 (1988) 3771.
[8] E. Adolfsson, P. Alberius-Henning, L. Hermansson, Phase analysis and thermal stability of hot isostatically pressed zirconia–hydroxyapatite composites, J. Am. Ceram. Soc. 83 (11) (2000) 2798.
[9] J. Li, H. Liao, L. Hermansson, Sintering of partially-stabilized zirconia and partially-stabilized zirconia–hydroxyapatite composites by hot isostatic pressing and pressureless sintering, Biomaterials 17 (1996) 1787.
[10] E. Adolfsson, L. Hermansson, Zirconia–fluorapatite materials produced by HIP, Biomaterials 20 (1999) 1263.
[11] V.V. Silva, R.Z. Domingues, Hydroxyapatite–zirconia composites prepared by precipitation method, J. Mater. Sci.: Mater. Med. 8 (1997) 907.

[12] K. Ioku, S. Somiya, M. Yoshimura, Hydroxyapatite ceramics with tetragonal zirconia particles dispersion prepared by HIP postsintering, J. Jpn. Ceram. Soc. 99 (1991) 196.
[13] Z. Evis, R.H. Doremus, Hot-pressed hydroxylapatite/monoclinic zirconia composites with improved mechanical properties, J. Mater. Sci. 42 (2007) 2426–2431.
[14] Z. Evis, C. Ergun, R.H. Doremus, Hydroxylapatite–zirconia composites: thermal stability of phases and sinterability as related to the $CaO–ZrO_2$ phase diagram, J. Mater. Sci. 40 (2005) 1127.
[15] Z. Evis, Reactions in hydroxylapatite–zirconia composites, Ceram. Int. 56 (2007) 987.
[16] H.W. Kim, Y.J. Noh, Y.J. Koh, H.E. Kim, H.M. Kim, Effect of CaF_2 on densification and properties of hydroxyapatite–zirconia composites for biomedical applications, Biomaterials 23 (2002) 4113.
[17] Z. Evis, M. Usta, I. Kutbay, Hydroxyapatite and zirconia composites: effect of MgO and MgF_2 on the stability of phases and sinterability, Mater. Chem. Phys. 110 (1) (2008) 68.
[18] Z. Evis, R.H. Doremus, Effect of YF_3 on hot-pressed hydroxyapatite and monoclinic zirconia composites, Mater. Chem. Phys. 105 (1) (2007) 76.
[19] Z. Evis, R.H. Doremus, Effect of ZrF_4 on hot-pressed hydroxyapatite/monoclinic zirconia composites, Scripta Mater. 56 (1) (2007) 53.
[20] A. Feinberg, C.H. Perry, Structural disorder and phase-transitions in $ZrO_2–Y_2O_3$ system, J. Phys. Chem. Solids 42 (1981) 513.
[21] T. Hirata, E. Asari, M. Kitajima, Infrared and Raman-spectroscopic studies of ZrO_2 polymorphs doped with Y_2O_3 or CeO_2, J. Solid State Chem. 110 (1994) 201.
[22] D.W. Lui, C.H. Perry, W. Wang, R.P. Ingel, Low-frequency Raman-spectra in disordered cubic zirconia at elevated-temperatures, J. Appl. Phys. 62 (1987) 250.
[23] D.I. Torres, J. Llopis, Infrared photoluminescence and Raman spectra in the $Y_2O_3–ZrO_2$ system, Superlattices Microstruct. 45 (2009) 482.
[24] K.J. Anusavice, J.A. Horner, C.W. Fairhurst, Adherence controlling elements in ceramic-metal systems. 1. Precious alloys, J. Dent. Res. 56 (9) (1977) 1045.
[25] K.J. Anusavice, J.A. Horner, C.W. Fairhurst, Interdiffusion behavior in porcelain fused to metal couples, J. Dent. Res. 56 (9) (1977) 1053.
[26] S.W. Pepper, Shear-strength of metal-sapphire contacts, J. Appl. Phys. 47 (1976) 801.